JOURNAL OF AGRICULTURAL AND FOOD CHEMISTRY

Article

pubs.acs.org/JAFC

Effects of Biomass Types and Carbonization Conditions on the Chemical Characteristics of Hydrochars

Xiaoyan Cao,[‡] Kyoung S. Ro,[§] Judy A. Libra,[⊥] Claudia I. Kammann,[⊗] Isabel Lima,[□] Nicole Berge,[△] Liang Li,[△] Yuan Li,[‡] Na Chen,[‡] John Yang,[○] Baolin Deng,[▽] and Jingdong Mao*[,†,‡]

[†]Department of Chemistry, College of Sciences, Nanjing Agricultural University, Nanjing 210095, People's Republic of China

[‡]Department of Chemistry and Biochemistry, Old Dominion University, 4541 Hampton Boulevard, Norfolk, Virginia 23529, United States

[§]Coastal Plains Soil, Water, and Plant Research Center, Agricultural Research Service, U.S. Department of Agriculture, 2611 West Lucas Street, Florence, South Carolina 29501, United States

[⊥]Leibniz Institute for Agricultural Engineering, Max-Eyth-Allee 100, 14469 Potsdam-Bornim, Germany

[⊗]Department of Plant Ecology, Justus-Liebig University Gießen, Heinrich-Buff-Ring 26-32 (IFZ), 35392 Giessen, Germany

[□]Southern Regional Research Center, Agricultural Research Service, U.S. Department of Agriculture, 1100 Robert E. Lee Boulevard, New Orleans, Louisiana 70124, United States

[△]Department of Civil and Environmental Engineering, University of South Carolina, Columbia, South Carolina 29208, United States

[○]Department of Agriculture and Environmental Science, Lincoln University of Missouri, Jefferson City, Missouri 65102, United States

[▽]Department of Civil and Environmental Engineering, University of Missouri, Columbia, Missouri 65211, United States

ABSTRACT: Effects of biomass types (bark mulch versus sugar beet pulp) and carbonization processing conditions (temperature, residence time, and phase of reaction medium) on the chemical characteristics of hydrochars were examined by elemental analysis, solid-state ^{13}C NMR, and chemical and biochemical oxygen demand measurements. Bark hydrochars were more aromatic than sugar beet hydrochars produced under the same processing conditions. The presence of lignin in bark led to a much lower biochemical oxygen demand (BOD) of bark than sugar beet and increasing trends of BOD after carbonization. Compared with those prepared at 200 °C, 250 °C hydrochars were more aromatic and depleted of carbohydrates. Longer residence time (20 versus 3 h) at 250 °C resulted in the enrichment of nonprotonated aromatic carbons. Both bark and sugar beet pulp underwent deeper carbonization during water hydrothermal carbonization than during steam hydrothermal carbonization (200 °C, 3 h) in terms of more abundant aromatic C but less carbohydrate C in water hydrochars.

KEYWORDS: *hydrochar, biomass type, lignin, process condition, chemical structure*

INTRODUCTION

There has been a recent surge in scientific research on applying carbonized biomass, in this context denoted "biochar", to soil, stimulated by its longevity and beneficial effects in Terra preta soils.[1−3] The applications of biochars to soils also provide a tool to reduce global warming by carbon sequestration.[4,5] The biochars used in most research have been produced via dry pyrolysis at temperatures >400 °C (pyrochars) from biomass with low water content.[6] In contrast, few studies have characterized products of the wet pyrolysis process, hydrothermal carbonization (HTC), which occurs at relatively low temperatures (180−350 °C) under autogenous pressures.[7,8] HTC proceeds by reactions including dehydration, decarboxylation, and recondensation and produces gases (predominantly CO_2), water-soluble organic substances, and carbon-rich solid residues referred to as hydrochars. The structures of hydrochars resemble those of natural lignite, but differ substantially from those of pyrochars.[9−12] Hydrochars generally contain less aromatic C because of their lower processing temperatures (180−350 °C), accounting for their lower recalcitrance to biodegradation when compared with pyrochars.[13,14] Recent research has identified several promising applications for hydrochars, for example, as functional carbon-based materials for catalysts, adsorbents, or energy storage, as potential soil amendments or peat substitute, or for carbon sequestration.[8,15−18]

The HTC process expands the range of potential feedstocks for char production to a variety of nontraditional, renewable, wet agricultural residues and municipal waste streams such as wet animal manures, municipal sewage, and solid waste, as well as industrial organic residues such as brewery spent grains or sugar beet pulp.[8,19] To determine suitable uses of these feedstocks for hydrochars, more information associated with the influence of feedstock properties on resulting hydrochar structure is necessary. Although considerable progress has been made recently toward understanding hydrochar structures by studying residues from HTC of well-defined substrates

Received: May 28, 2013
Revised: August 31, 2013
Accepted: September 4, 2013
Published: September 4, 2013

Table 1. Chemical Composition of Selected Potential Feedstocks for HTC

	% dry weight of total solids					
composition	sugar beet pulp[a]	spruce bark[b]	spruce wood[b]	cattle manure (dairy/beef)[c]	swine manure[c]	poultry manure[c]
lignin	1−6	10−20	40−45	12−13	4−6	2−7
cellulose	20−24	15−20	20−25	22−27	13−14	8−12
hemicellulose	25−36	15−20	25−30	12−17	20−22	16−22
protein	7−11			12−18	22−25	28−44
pectin	19−25					
sucrose	4					
minerals/ash	4	2−5	3−4			
extractives		20−30	0.2−0.6			

[a]Data from Sutton and Peterson.[36] [b]Data from Kraft.[37] [c]Data from Chen et al.[38]

(glucose, cellulose, sucrose, starch, etc.),[15,16,20−22] the hydrochar structures derived from heterogeneous waste substrates are much less understood.[11,19,21,23] These materials commonly contain significant amounts and differing fractions of cellulose, hemicellulose, proteins, and lignin (Table 1). The complexity of these feedstocks likely influences resulting hydrochar properties. Cellulose is solubilized and removed from biomass during HTC, forming, for example, hydrochars with spherical structures. Lignin is scarcely decomposed, however, resulting in a hydrochar with a strongly porous framework, often with the outer contours of the initial material.[24,25] In addition to the hydrochar diversity expected due to different feedstock compositions, HTC process conditions (e.g., temperature and residence time) and the phase of reaction medium such as steam or liquid water can be varied, possibly leading to even more variations in the physical and chemical properties of produced hydrochars. As such, structural variations in hydrochar induced by different feedstock types and processing conditions may play an important role in its biodegradability, stability, and functionality in various applications.

In the present study, HTC was applied to two common waste feedstocks: bark peel (used as mulch in gardening) and sugar beet pulp, with various compositions (Table 1). The objectives were to investigate the effects of (1) the presence or absence of lignin in feedstocks and (2) processing variables (temperature, time, and reaction medium) on hydrochar structures using elemental analysis, advanced solid-state ^{13}C NMR, and common tests for biodegradability, chemical and biochemical oxygen demand (COD and BOD). This represents the first attempt in the literature to characterize hydrochars prepared in the presence of steam. A better understanding of hydrochar characteristics as a result of feedstock types and processing variables achieved in this study will provide a basis for maximizing the potential use of hydrochars.

MATERIALS AND METHODS

Hydrochar Preparation. Two steam hydrochars (S-HTC) and six water hydrochars (W-HTC) were prepared from the feedstocks, bark mulch and sugar beet pulp (referred to as bark and sugar beet in the following sections). The process conditions (temperature and time) can be summarized as follows: S-HTC-bark/S-HTC-beet (200 °C, 3 h), W-HTC-bark/W-HTC-beet (200 °C, 3 h), W-HTC-bark/W-HTC-beet (250 °C, 3 h), and W-HTC-bark/W-HTC-beet (250 °C, 20 h).

The patented hydrothermal carbonization in the steam medium (Revatec GmbH, DE 10 2009 010 233.7) was conducted in a 70 L stainless steel reactor. The feedstocks (chipped sugar beet pulp, 1.0−1.5 cm; and shredded bark, <5 cm) with moisture contents of about 40−70% were placed in the reactor. No additional water was required. The reactor system utilizes steam to maintain a pressure at the required set point, 16 bar for 3 h at 200 °C. Any steam condensates were drained from the reactor. No extra dewatering of the S-HTC hydrochars was undertaken, and the samples were dried for storage.

The hydrothermal carbonization in the water medium was conducted in a 1 L non-stirred T316 stainless steel vessel with an external heater. The dried and ground (<2 mm) sugar beet or bark was added along with distilled water to the reactor to obtain a solid concentration of 20% (wt). The reactor was heated to the desired reaction temperature (200 or 250 °C) with a heating rate of about 7 °C/min. The reactor temperature was maintained under its autogenic pressure for the desired reaction time (3 or 20 h). Afterward, the reactor was cooled to room temperature before the reaction products were filtered and dried at 100 °C.

Chemical Properties. Proximate analyses for all samples were performed in duplicate, following American Society for Testing and Materials (ASTM) method D5142[26] using a LECO thermogravimetric analyzer (TGA701, LECO, St. Joseph, MI, USA). Percent moisture was determined as the weight loss after the samples had been heated in an open crucible to 107 °C and held at this temperature until constant weight, in a flow of nitrogen. The percent volatile matter was determined as the weight loss after the samples had been heated in covered crucibles to 950 °C and held for 7 min under a flow of nitrogen. Ash content was defined as the remaining mass after subsequent heating under a flow of oxygen, in open crucibles to 750 °C and holding at this temperature until sample weight was constant. After the determination of moisture, ash, and volatile matter, the fixed carbon content was calculated by difference.

NMR Spectroscopy. ^{13}C NMR analyses were performed using a Bruker Avance III 300 spectrometer at 75 MHz (300 MHz ^{1}H frequency). All experiments were run in a double-resonance probe head using 4 mm sample rotors. The NMR experimental details can be found elsewhere.[27] The ^{13}C chemical shifts were referenced to tetramethylsilane, using the COO resonance of glycine in the α-modification at 176.46 ppm as a secondary reference.

Quantitative ^{13}C direct polarization/magic angle spinning (DP/MAS) NMR experiments were performed at a spinning speed of 13 kHz. The 90° ^{13}C pulse length was 4 μs. Recycle delays were determined by the cross-polarization/spin−lattice relaxation time/total sideband suppression (CP/T_1-TOSS) technique to ensure all carbon nuclei were relaxed by >95%. The ^{13}C DP/MAS NMR with recoupled dipolar coupling (DP/MAS/DD) was used to quantify the nonprotonated carbons and mobile carbon fractions. The dipolar dephasing time was 68 μs. The number of scans for DP/MAS and DP/MAS/DD experiments for all samples was 1024.

Semiquantitative compositional information was obtained with good sensitivity using a ^{13}C CP/MAS NMR technique with MAS 5 kHz, CP time 1 ms, and ^{1}H 90° pulse length 4 μs. Four-pulse total suppression of sidebands (TOSS)[28] was employed before detection, with two-pulse phase-modulated decoupling applied for optimum resolution. Subspectra for nonprotonated and mobile carbon groups were obtained by combining the ^{13}C CP/TOSS sequence with a 40 μs dipolar dephasing (CP/TOSS/DD). The number of scans for ^{13}C CP/TOSS and ^{13}C CP/TOSS/DD experiments was 6144 for all samples.

Table 2. Proximate and Ultimate Analyses of Feedstocks and Hydrochars[a]

	wt %								
sample	MC	VM_{db}	FC_{db}	ash_{db}	C_{daf}	H_{daf}	N_{daf}	S_{daf}	O_{daf}
sugar beet	6.9 ± 0.01	75.4 ± 0.3	18.5 ± 0.2	6.2 ± 0.2	51.1 ± 0.2	6.7 ± 0.9	3.4 ± 0.02	0.2 ± 0.04	38.7 ± 1.0
S-HTC-beet (200 °C, 3 h)	4.6 ± 0.02	61.0 ± 0.4	32.0 ± 0.3	7.1 ± 0.3	67.3 ± 1.0	3.6 ± 0.9	4.2 ± 0.1	0.1 ± 0.01	24.8 ± 1.9
W-HTC-beet (200 °C, 3 h)	4.1 ± 0.1	66.2 ± 0.4	21.2 ± 0.5	12.6 ± 0.8	61.3 ± 0.5	5.4 ± 0.8	5.3 ± 0.6	0.1 ± 0.01	27.8 ± 1.3
W-HTC-beet (250 °C, 3 h)	4.7 ± 0.2	51.8 ± 0.9	35.7 ± 1.0	12.5 ± 0.2	71.1 ± 2.0	7.6 ± 0.1	1.7 ± 0.3	0.9 ± 0.1	17.1[b] ± 0.4
W-HTC-beet (250 °C, 20 h)	3.9 ± 0.03	50.0 ± 0.3	38.1 ± 0.2	12.0 ± 0.1	72.2 ± 2.0	7.1 ± 0.3	2.7 ± 0.1	1.2 ± 0.1	18.0[b] ± 1.5
bark	7.0 ± 0.1	66.8 ± 0.4	25.5 ± 0.3	7.7 ± 0.2	59.8 ± 2.0	6.3 ± 0.7	1.2 ± 0.2	0.1 ± 0.02	32.6 ± 1.3
S-HTC-bark (200 °C, 3 h)	6.0 ± 0.1	56.1 ± 0.3	37.3 ± 0.1	6.6 ± 0.2	69.0 ± 1.9	3.1 ± 0.7	1.5 ± 0.2	0.1 ± 0.02	26.3 ± 1.5
W-HTC-bark (200 °C, 3 h)	10.0 ± 0.1	60.2 ± 1.4	35.1 ± 0.3	4.7 ± 1.2	64.4 ± 0.5	6.6 ± 1.3	1.4 ± 0.2	0.1 ± 0.02	27.5 ± 1.1
W-HTC-bark (250 °C, 3 h)	3.7 ± 0.02	50.6 ± 0.3	43.2 ± 0.5	6.2 ± 0.8	70.8 ± 1.2	6.1 ± 0.4	0.1 ± 0.1	0.6 ± 0.04	21.3[b] ± 0.9
W-HTC-bark (250 °C, 20 h)	4.4 ± 0.2	45.2 ± 1.2	46.9 ± 0.7	7.9 ± 1.9	72.2 ± 1.5	6.0 ± 1.3	0.4 ± 0.1	0.7 ± 0.3	17.7[b] ± 2.0

[a]MC, moisture content; VM, volatile matter; FC, fixed C; db, dry basis; daf, dry ash free basis. [b]Calculated using a depletion method after C, H, N, and S values.

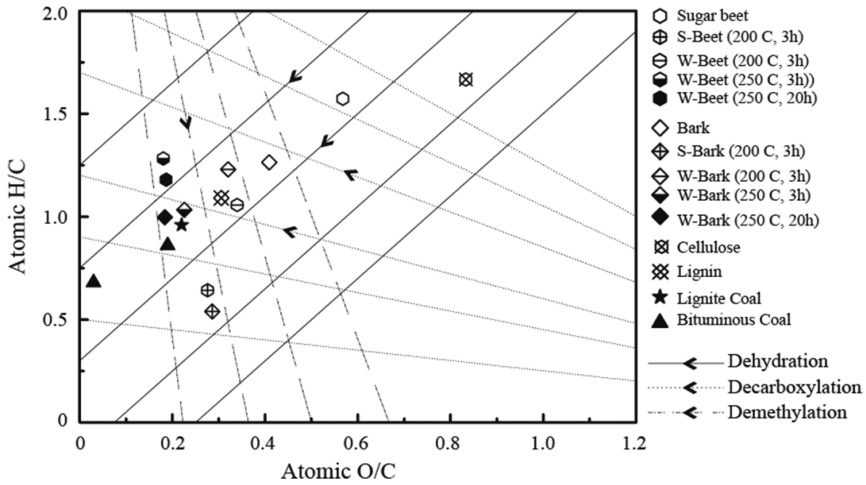

Figure 1. Atomic H/C and O/C ratios of the feedstocks and hydrochars resulting from hydrothermal carbonization. The atomic ratios for cellulose, lignin,[24] and bituminous and lignite coals[19] are included for comparative purposes.

Because O−C−O carbons (e.g., anomeric C in carbohydrate rings) and aromatic carbon resonances between 120 and 90 ppm are difficult to resolve, the aromatic carbon signals were selectively suppressed using a five-pulse ^{13}C chemical shift anisotropy (CSA) filter with a CSA filter time of 47 μs. The number of scans was 6144 for all samples.

Spectra for immobile CH_2 + CH groups were obtained using the following spectral-editing techniques. First, a ^{13}C CP/TOSS spectrum was recorded using a short CP time (50 μs) to emphasize protonated carbons in immobile segments. Afterward, a second ^{13}C CP/TOSS spectrum was recorded using a short CP (50 μs) coupled with a 40 μs dipolar dephasing. The difference spectrum represents immobile CH_2 and CH carbons, with a small CH_3 contribution. The number of scans was 6144 for all samples.

The size of fused aromatic rings was estimated from the recoupled $^1H-^{13}C$ dipolar dephasing. In short, two ^1H 180° pulses per rotation period prevent MAS from averaging out weak CH dipolar couplings. To detect nonprotonated carbons with good relative efficiency, direct polarization/total sideband suppression (DP/TOSS) was used at a spinning rate of 7 kHz. The ^{13}C 90° and 180° pulse lengths were 4 and 8 μs, respectively. The number of scans was 640 for all samples at each dephasing time.

Chemical and Biochemical Oxygen Demand Measurements of Hydrochars. The COD and 5 day BOD of hydrochar suspensions were measured. Hydrochar samples were ground for 30 s in an analytical mill (A 11, IKA) to increase sample homogeneity. Subsequently, the ground hydrochars were mixed in deionized water to obtain suspensions with a solid concentration of approximately 3000 mg/L. All suspensions were shaken for 16 h in a rotary shaker. Following shaking, well-mixed samples were taken and analyzed for COD and BOD. Suspension COD was measured using HACH reagents (HR test kit, Loveland, CO, USA) and conducted in triplicate. Suspension BOD (5 day) was measured using a respirometric technique (BODTrak II, HACH) and also conducted in triplicate.

RESULTS AND DISCUSSION

Elemental Composition of Hydrochars. The analysis of the composition of feedstocks and hydrochars showed that fixed carbon (FC) content increased while volatile matter (VM) decreased as the reaction temperature and residence time

dx.doi.org/10.1021/jf402345k | J. Agric. Food Chem. 2013, 61, 9401−9411

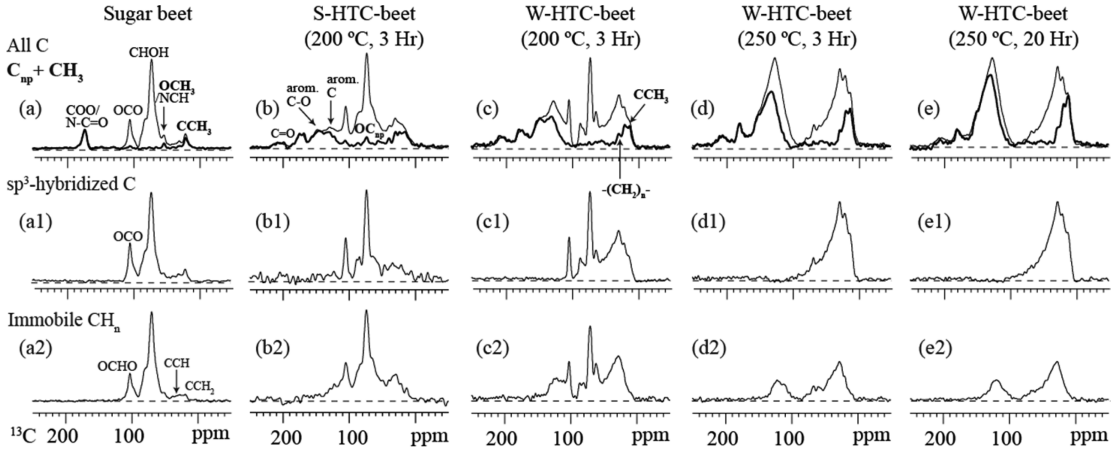

Figure 2. ^{13}C NMR spectral editing for identification of functional groups in sugar beet and their hydrochars: (a–e) thin lines, unselective CP/TOSS spectra; thick lines, corresponding dipolar-dephased CP/TOSS spectra; (a1–e1) selection of sp³-hybridized C signals by a ^{13}C CSA filter; (a2–e2) selection of relatively immobile CH and CH_2 signals with small residual CH_3, achieved by the difference between a short CP spectrum and a spectrum of short CP combined with dipolar dephasing.

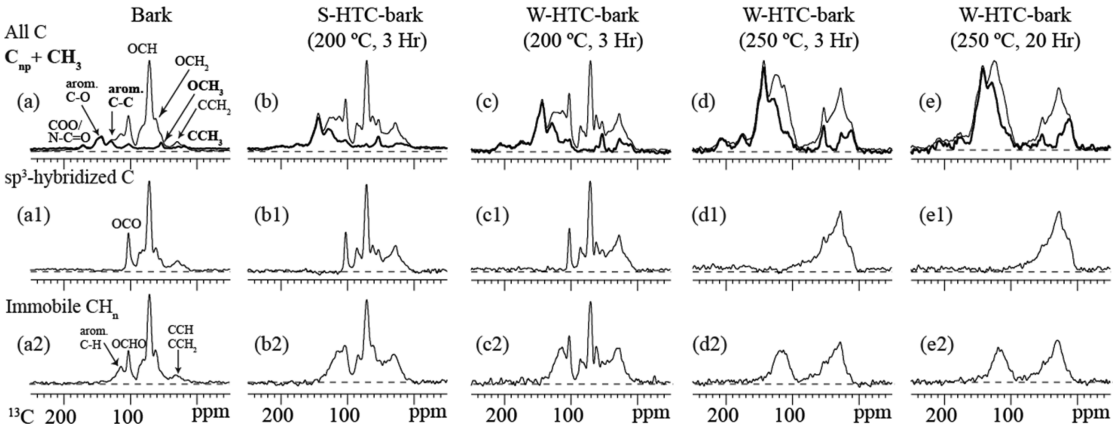

Figure 3. ^{13}C NMR spectral editing for identification of functional groups in bark and their hydrochars: (a–e) thin lines, unselective CP/TOSS spectra; thick lines, corresponding dipolar-dephased CP/TOSS spectra; (a1–e1) selection of sp³-hybridized C signals by a ^{13}C CSA filter; (a2–e2) selection of relatively immobile CH and CH_2 signals with small residual CH_3, achieved by the difference between a short CP spectrum and a spectrum of short CP combined with dipolar dephasing.

increased (Table 2). Ash content trended upward in sugar beet hydrochars, but did not change much in bark hydrochars. The C content of the hydrochars increased with processing time and temperature for both feedstocks in water medium (Table 2). The increase of C contents in steam hydrochars relative to feedstocks (S-HTC-beet, 16.2%; S-HTC-bark, 9.2%) was more evident than in corresponding water hydrochars (W-HTC-beet, 10.2%; W-HTC-bark, 4.6%) prepared at 200 °C for 3 h. The mechanisms associated with this increase are currently unknown. As expected, the O content of water hydrochars decreased with processing time and temperature. The carbonization resulted in slightly lower O contents of hydrochars in steam than those prepared in water medium at the same temperature and processing time. The HTC processing of both sugar beet and bark led to slight changes of H in their water hydrochars, but lower H content in steam hydrochars. The N content was higher in the sugar beet feedstock than in the bark and remained higher in the respective hydrochars. Although the N contents were lower in the hydrochars produced at the higher temperature (250 °C), they showed no clear trend with temperature and time. In contrast, the sulfur contents, which were also relatively low (<1.2%) in all samples, increased with temperature and time.

The elemental compositions of chars and coals are often visualized by a van Krevelen diagram plotting H/C versus O/C atomic ratios.[29] The H/C and O/C ratios serve as indicators for the degree of carbonization of hydrochars. High ratios indicate the presence of primary plant macromolecules (i.e., cellulose), whereas low ratios are typical of more condensed (aromatic) structures.[14,30] Sugar beet feedstock appeared within the typical carbohydrate region, but shifted to relatively lower O/C (~0.6) than cellulose (Figure 1). Bark feedstock had H/C and O/C ratios much lower than cellulose and sugar beet, but higher than lignin, consistent with its composition. Steam and water hydrochars produced from bark and sugar beet all shifted to lower H/C and O/C values due to carbonization. They had H/C ratios ranging from 0.6 to 1.3, and O/C ratios exhibiting smaller variations from 0.2 to 0.4, consistent with previous results.[14] The H/C ratios remained lower in bark hydrochars than in the corresponding sugar beet hydrochars prepared under the same conditions, but their O/C ratios became very similar. The surprisingly higher H/C of W-HTC-bark relative to W-HTC-beet hydrochars prepared at 200 °C for 3 h might

dx.doi.org/10.1021/jf402345k | J. Agric. Food Chem. 2013, 61, 9401–9411

be explained by uncharred residues of primary plant macromolecules such as cellulose in bark water hydrochars.[30] The locations of hydrochars on the plot further depended on process parameters (temperature, time, and reaction medium). For example, both sugar beet and bark steam hydrochars showed markedly lower H/C (0.5−0.6) than their corresponding water hydrochars with H/C (1−1.2) prepared at the same temperature and reaction time (200 °C, 3 h). This suggested that steam HTC leads to more condensed structures (low H/C) than water HTC following common interpretation of van Krevelen diagram.[14] As the HTC temperature increased from 200 to 250 °C, the O/C atomic ratios decreased in both sugar beet and bark hydrochars. However, the H/C atomic ratio showed different trends. It decreased for bark hydrochars but increased for sugar beet hydrochars. It appears that dehydration was more intense at 250 °C for conversion of bark than at 200 °C, whereas decarboxylation was more intense at 250 °C for the conversion of sugar beet than at 200 °C (Figure 1). Further increasing reaction time from 3 to 20 h led to lower H/C ratios in sugar beet hydrochars and slightly decreased O/C ratios in bark hydrochars. Overall, as the HTC reaction intensity increased, that is, higher temperatures and longer reaction times, the resulting hydrochars became increasingly similar to lignite.

Detailed NMR Analyses of Hydrochars Based on Spectral-Editing Techniques. Figures 2 and 3 show the spectra from ^{13}C cross-polarization/total sideband suppression (CP/TOSS) and spectral editing experiments of sugar beet, bark, and their hydrochars prepared under different conditions. Top spectra (Figures 2a−e and 3a−e) are ^{13}C CP/TOSS spectra (thin lines) showing signals from all C sites and ^{13}C cross-polarization/total sideband suppression with dipolar dephasing (CP/TOSS/DD) spectra (thick lines) highlighting signals from nonprotonated C and mobile groups.

The CP/TOSS spectrum of sugar beet feedstock (Figure 2a, thin line) exhibited exclusively signals characteristic of cellulose/hemicellulose, such as those from *O*-alkyl C (62, 72, and 82 ppm), di-*O*-alkyl C (103 ppm), and CH_3COO (18 and 173 ppm). As compared to that of sugar beet feedstock, the CP/TOSS spectrum of its steam hydrochar (Figure 2b, thin line) showed (1) overlapping of alkyl, *O*-alkyl, and di-*O*-alkyl C bands; (2) relative enrichment of alkyl C; and (3) evolution of signals from aromatic C−C/C−H (112−150 ppm) and aromatic C−O (150−165 ppm). The CP/TOSS spectrum of W-HTC-beet (Figure 2c, thin line) differed from that of S-HTC-beet in that intensities of signals from alkyl C, aromatic C−C/C−H, and aromatic C−O were much higher in W-HTC-beet. The spectra of water hydrochars produced at 250 °C for 3 and 20 h (Figure 2d,e) were quite similar and resembled those of lignite, but were distinct from those of S-HTC-beet and W-HTC-beet at 200 °C. They exhibited dominant signals from nonpolar alkyl (0−48 ppm) and aromatic C (90−165 ppm). Other minor signals from OCH (72 ppm), COO/NC═O (165−190 ppm), and ketone/aldehyde C (190−220 ppm) were slightly more abundant in W-HTC-beet (250 °C, 3 h) than in W-HTC-beet (250 °C, 20 h). The dipolar-dephased CP/TOSS spectrum of sugar beet (Figure 2a, thick line) clearly selected signals of CH_3 and COO/N—C═O, as well as tiny signals of OCH_3, likely assigned to methyl esters in pectin. The dipolar-dephased spectra of the S-HTC-beet and W-HTC-beet (200 °C, 3 h) (Figure 2b,c, thick lines) both displayed signals from CH_3, mobile $(CH_2)_n$, OCH_3, nonprotonated *O*-alkyl, aromatic C−C, aromatic C−O, COO/NCO, and ketone/aldehyde C, but the intensities of these signals were different for the two hydrochars. Among those, the signals of aromatic C−C and CH_3 were further enhanced in the spectra of W-HTC-beet (250 °C, 3 h; 250 °C, 20 h) (Figure 2d,e, thick lines), but those from carbohydrates were almost removed. Although the spectrum of sugar beet showed a single peak at ∼22 ppm for CH_3, those of sugar beet hydrochars exhibited two distinct peaks at ∼17 and ∼22 ppm of CH_3, respectively, representing the CH_3 groups in two different chemical environments.

The CSA-filtered spectra selected the resonances of sp^3-hybridized C and resolved the di-*O*-alkyl peak in the spectra of S-HTC-beet and W-HTC-beet prepared at 200 °C for 3 h (Figure 2b1,c1). The residual signals of OCH and other *O*-alkyls were still observable, but di-*O*-alkyl resonances were clearly absent in the spectra of hydrochars prepared at 250 °C (Figure 2d1,e1). Therefore, there were no carbohydrates in the hydrochars prepared at 250 °C. The protonated C-only spectrum of sugar beet showed signals primarily from OCHO, CHOH, CH_2OH, CCH, CCH_2, and CCH_3. Those of S-HTC-beet and W-HTC-beet (200 °C, 3 h) (Figure 2b2,c2) clearly showed aromatic C−H signals at 112−140 ppm, with their intensities much more prominent in W-HTC-beet (200 °C, 3 h). For the hydrochars produced at 250 °C, the immobile CH_n spectra (Figure 2d2,e2) were dominated mainly by resonances of aromatic C−H and aliphatic CCH, CCH_2C, and remaining protonated *O*-alkyl C.

The CP/TOSS and CP/TOSS/DD spectra of bark feedstock (Figure 3a) showed peaks characteristic of lignocellulosic biomass, that is, signals from (1) cellulose/hemicellulose and (2) lignin including $ArOCH_3$ (57 ppm), OCH (C_β of lignin, 82 ppm), aromatic C (110−140 ppm), and oxygenated aromatic C (148 ppm). The CP/TOSS and CP/TOSS/DD spectra of bark steam hydrochar (Figure 3b) as compared to those of bark feedstock showed (1) enrichment of signals from CH_3, CH_2, OCH_3 and aromatic C (protonated, nonprotonated, and oxygenated), relative to those associated with carbohydrates, and (2) the appearance of a small broad signal around 206 ppm assigned to ketone/aldehyde C. These spectral variations were more pronounced in the water hydrochars treated at 200 °C for 3 h (Figure 3c). The peaks attributed to carbohydrates almost disappeared in the CP/TOSS spectra of water hydrochars produced at 250 °C (Figure 3d,e), whereas nonpolar alkyl and aromatic resonances dominated these spectra. Their dipolar-dephased spectra still showed distinct signals of aromatic C−O, aromatic C−C, and OCH_3 indicative of the preservation of lignin due to its higher temperature-resistance.

Panels a1−e1 of Figure 3 exhibit CP/TOSS spectra after the insertion of the ^{13}C CSA filter of bark feedstock and its hydrochars. The di-*O*-alkyl C signal was distinct in the spectra of bark, S-HTC-bark, and W-HTC-bark (200 °C, 3 h) (Figure 3a1−c1), but absent in those of hydrochars prepared at 250 °C (Figure 3d1,e1), suggestive of a lack of carbohydrates. The protonated C-only spectra of bark feedstock, and its steam and water hydrochars prepared at 200 °C (Figure 3a2−c2) showed signals primarily from aromatic C−H, OCHO, CHOH, CH_2OH, CCH, and CCH_2. Among those, the signals from aromatic C−H, CCH, and CCH_2 were more enriched in the spectra of S-HTC-bark and W-HTC-bark (200 °C, 3 h). For water hydrochars produced at 250 °C, the immobile CH_n (or protonated-C-only) spectra (Figure 3d2,e2) were dominated mainly by resonances of aromatic C−H and aliphatic CCH and CCH_2.

dx.doi.org/10.1021/jf402345k | J. Agric. Food Chem. 2013, 61, 9401−9411

Quantitative Structural Composition of Hydrochars Based on DP NMR. Quantitative chemical compositions of feedstocks and hydrochars were reliably obtained from DP spectra. Figure 4 presents the spectra of ^{13}C DP/MAS (thin lines) and ^{13}C DP/MAS with 68 μs recoupled dipolar dephasing (thick lines) of all samples. Comparison with corresponding CP spectra clearly reveals the overestimation of signals of protonated C in CP spectra. Relative intensities of C functional groups in all samples based on DP spectra can be found in Table 3. The distribution of major C functional groups is more clearly shown in Figure 5.

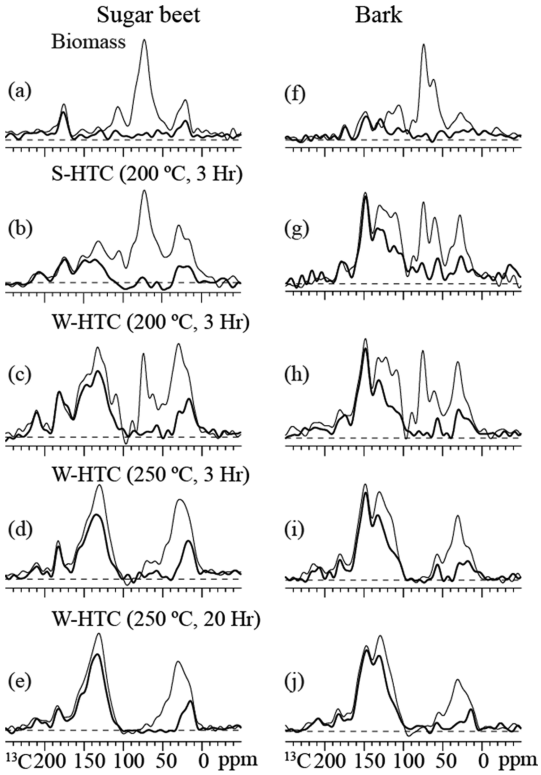

Figure 4. Quantitative ^{13}C DP/MAS NMR spectra (thin lines) and DP/MAS after recoupled dipolar dephasing showing nonprotonated carbons plus mobile groups such as CH_3 (thick lines). Spectra are scaled to match the intensity of the highest band.

According to Figure 5 and Table 3, the dominant component in the sugar beet was carbohydrates (*O*-alkyl), accounting for 77% of total C, followed by alkyl C (13%) and OCH_3/NCH (8%). The contribution of NCH is estimated to be at most 5−6% of all C on the basis of a C/N ratio of 17.5 for sugar beet. Compared with sugar beet, the steam hydrochar contained much fewer carbohydrates (34%). Alkyl C became enriched (25%), COO/N—C═O also increased (7%), but OCH_3/NCH decreased to 6%. New C forms were formed, including aromatic C−C (12%), aromatic C−H (7%), aromatic C−O (5%), and ketones/aldehydes (5%). The dominant component in water hydrochar (200 °C, 3 h) was aromatic C (37%), followed by alkyl C (28%), *O*-alkyl C (17%), COO/N—C═O (9%), ketones/aldehydes (5%), and OCH_3/NCH (4%). For the water hydrochars prepared at 250 °C for 3 and 20 h, aromatics comprised 48 and 53%, alkyl C comprised 36 and 32%, COO/N—C═O comprised 7 and 7%, and aldehyde/ketone C comprised 4 and 5%, respectively. These two hydrochars contained only 3 and 1% of *O*-alkyl C, respectively.

Although carbohydrate C (50%) was the major component in the bark feedstock, it also contained abundant aromatics (23%), alkyl (16%), OCH_3/NCH (9%), and COO/N—C═O (3%). By contrast, the steam hydrochar prepared at 200 °C became dominant in aromatics (42%), followed by *O*-alkyl C (27%), alkyl C (18%), OCH_3/NCH (6%), COO/N—C═O (4%), and aldehyde/ketone (2%). Compared to steam hydrochar, corresponding water hydrochar (200 °C, 3 h) contained slightly more aromatics (45%), COO/N—C═O (6%), and aldehyde/ketone (4%), but less *O*-alkyl C (23%) and OCH_3/NCH (4%). For hydrochars prepared at 250 °C for 3 and 20 h, aromatics accounted for 61 and 63%, followed by alkyl C (22 and 21%), COO/N—C═O (7 and 7%), aldehyde/ketone (5 and 4%), and OCH_3/NCH (4 and 3%). Carbohydrate C comprised only ∼1% of all C in hydrochars prepared at 250 °C.

Several major findings from CP and DP data were as follows: (1) Whereas sugar beet feedstock was predominantly composed of carbohydrates, bark also consisted of lignin in

Table 3. Composition of Functional Groups (Percent) in Biomass and Different Hydrochars Obtained by Quantitative DP/NMR Analyses

	220−190 ppm	190−165 ppm	165−150 ppm[a]	150−112 ppm[a]		112−60 ppm[a]	60−48 ppm	48−0 ppm
sample	aldehyde/ketone	COO/N—C═O	arom C—O	arom C—C	arom C—H	*O*-alkyl	O—CH_3/ NCH	alkyl
sugar beet	0	1	0	0	0	77	8	13
S-beet (200 °C/3 h)	5	7	5	12	7	34	6	25
W-beet (200 °C/3 h)	5	9	7	21	9	17	4	28
W-beet (250 °C/3 h)	4	7	7	29	12	3	3	36
W-beet (250 °C/20 h)	5	7	9	33	11	1	3	32
bark	0	3	10	9	4	50	9	16
S-bark (200 °C/3 h)	2	4	18	15	9	27	6	18
W-bark (200 °C/3 h)	4	6	20	15	10	23	4	19
W-bark (250 °C/3 h)	5	7	25	23	13	1	4	22
W-bark (250 °C/20 h)	4	7	25	27	11	1	3	21

[a]Note that for hydrochars prepared at 250 °C, the spectral range of 90−140/150 ppm is assigned to aromatic C, and 60−90 ppm is assigned to O-alkyl C. For beet and beet hydrochars, the spectral range of 112−140 ppm is assigned to aromatic C−C and aromatic C−H, and that of 140−165 ppm is assigned to aromatic C−O. Sidebands are corrected and added to the centerband on the basis of methods provided by Mao and Schmidt-Rohr.[39] The percentages in each row add up to 100.

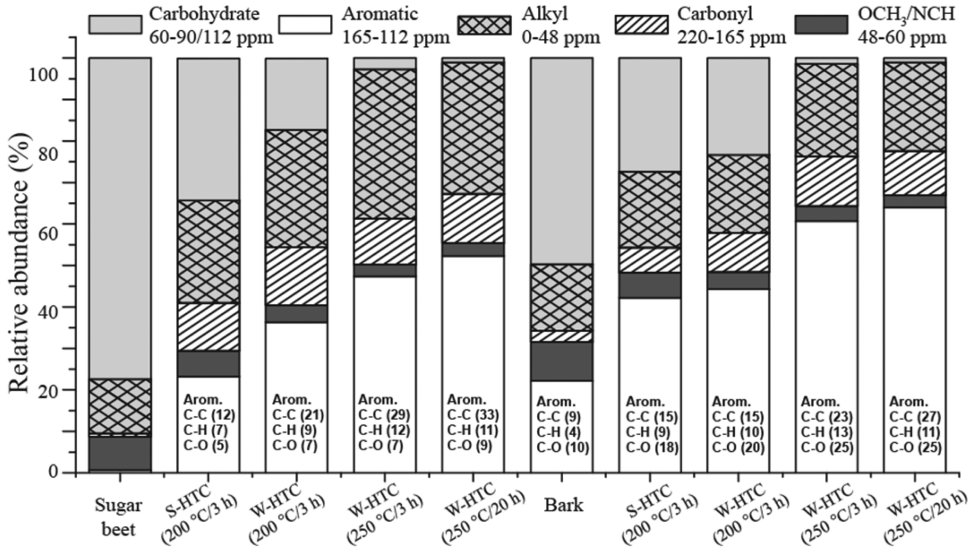

Figure 5. Distribution of major C functional groups in sugar beet, bark, and their hydrochars.

addition to cellulose/hemicellulose. (2) The HTC processing of sugar beet and bark led to the depletion of carbohydrate C and OCH_3/NCH and formation and/or enrichment of aromatic C, as well as increase of alkyl and carbonyl C. (3) Carbohydrate structures were evident in the steam and water hydrochars prepared at 200 °C, but almost completely removed in the 250 °C hydrochars. (4) Carbohydrates were more abundant in W-HTC-bark than in W-HTC-beet prepared at 200 °C for 3 h. This supported our previous explanation that the higher H/C of W-HTC-bark relative to W-HTC-beet may arise from uncharred residues of primary plant macromolecules such as cellulose. (5) Lignin structures were preserved or altered to a limited extent in the bark hydrochars. (6) Finally, water hydrochars produced from sugar beet and bark (especially sugar beet) at 200 °C for 3h contained more aromatic C, COO/NC═O, and alkyl C, but less carbohydrate C and OCH_3/NCH, than corresponding steam hydrochars, suggesting that feedstocks undergo deeper carbonization in the water medium than in the steam medium. Finding 6 is seemingly inconsistent with the common interpretation of the results from elemental analysis (Figure 1).[14] The steam hydrochars from both bark and sugar beet showed H/C values of ~0.6, much lower than their corresponding water hydrochars, suggesting a higher degree of condensation in the structures of steam hydrochars. This is discussed further below.

Aromatic Structures in Hydrochars. ^{13}C NMR analyses in the present and previous studies have shown that aromatic C is formed (i.e., sugar beet hydrochars) and/or enriched (i.e., bark hydrochars) after HTC processing, but there have been doubts as to whether aromatic C is present within six-membered benzene- or furan-based structures.[15,16,20−22,31] The NMR spectra of sugar beet and bark hydrochars in the present study showed a central aromatic peak at 130 ppm, whereas peaks characteristic of a furanic ring (150 and 110−118 ppm) were absent. This is consistent with our previous study[23] and supports the benzene ring-based hydrochar models.[15,16,21,22] In the case of bark hydrochars, the lignin fraction in the starting biomass was relatively unaffected and preserved as part of aromatic C.

Although it is commonly accepted that chars from dry pyrolysis (>400 °C) consist of highly condensed aromatic clusters, the extent of polyaromatic hydrocarbons inside hydrochars has remained unclear (separate single ring versus fused aromatic clusters). For this purpose, long-range $^{1}H-^{13}C$ dipolar dephasing experiments were performed on the water hydrochars prepared at 250 °C. Those hydrochars prepared at 200 °C were not analyzed because their structures still contained significant features of biomass, with fewer aromatic C atoms. The dephasing rate curves of the aromatic C of the four hydrochars, as well as those of lignin and swine manure-derived hydrochar,[23,32] are shown in Figure 6. The curves for specific sites in model compounds (C-1 of 3-methoxybenzamide and C-11 of 1,8-dihydroxy-3-methylanthraquinone, structures shown in Figure 6), with two two-bond and three

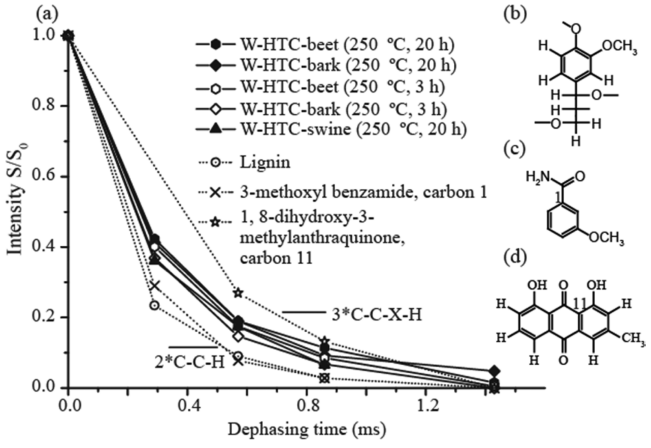

Figure 6. Plot of the area of signals of aromatic carbons in hydrochars and model compounds versus dephasing time. (a) Plot of the area of signals of aromatic carbons resonating between 107 and 142 ppm versus dephasing time: ⬢, W-HTC-beet (250 °C, 20 h); ◆, W-HTC-bark (250 °C, 20 h); ⬡, W-HTC-beet (250 °C, 3 h); ◇, W-HTC-bark (250 °C, 3 h); ▲, W-HTC-swine (250 °C, 20 h); ○, lignin; ×, carbon 1 of 3-methoxybenzamide, which is two bonds away from the two nearest protons; ☆, carbon 11 of 1,8-dihydroxy-3-methylanthraquinone, which is three bonds away from the three nearest protons. The data points have been corrected for regular T_2 relaxation. (b) Structure of a typical softwood-lignin unit. (c) Structure of 3-methoxybenzamide and carbon numbering. (d) Structure of 1,8-dihydroxy-3-methylanthraquinone and carbon numbering.

dx.doi.org/10.1021/jf402345k | J. Agric. Food Chem. 2013, 61, 9401−9411

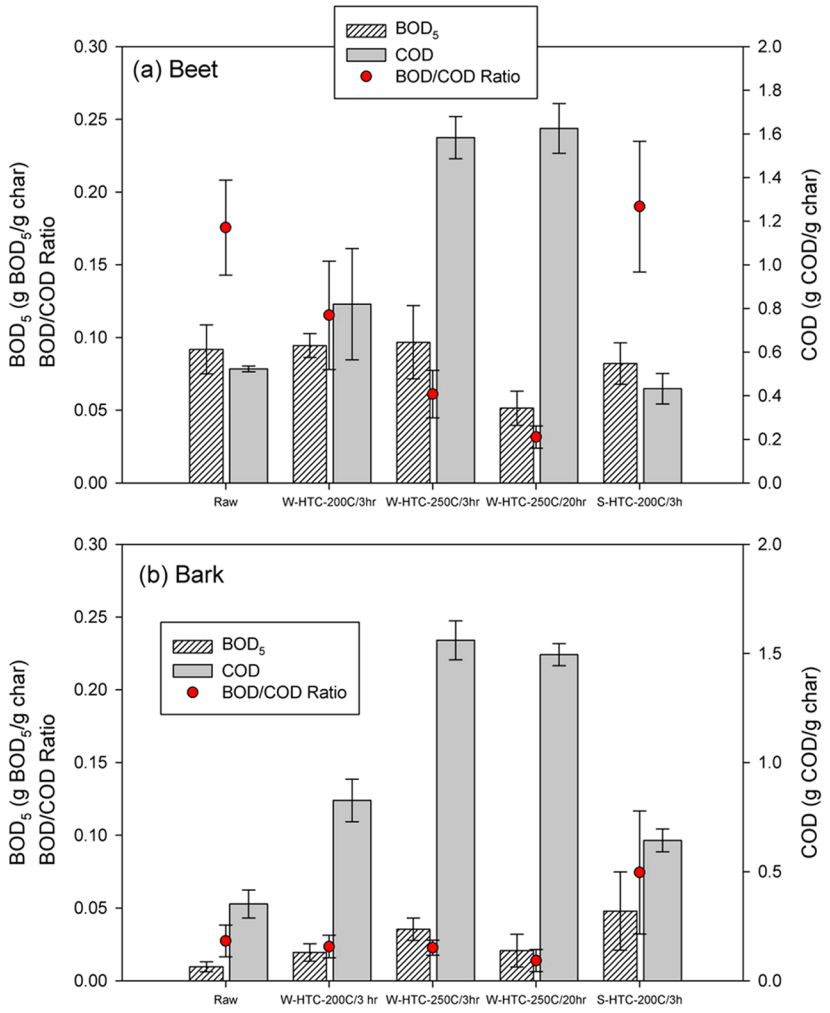

Figure 7. BOD, COD, and BOD/COD ratio associated with hydrochars resulting from the carbonization of (a) sugar beet and (b) bark. Error bars represent measurement standard deviations.

three-bond couplings, respectively, provide an approximate length-scale calibration. The dephasing curves of sugar beet and bark hydrochars nearly coincided with each other and with previously analyzed swine manure hydrochar. In addition, the dephasing rates of these hydrochars were slower than that of lignin or the two-bond model, but faster than that of the three-bond model. Overall, our results indicated (1) a similar extent of aromatic condensation of hydrochars prepared at 250 °C regardless of source materials and reaction time; (2) more condensed or substituted aromatic rings in 250 °C hydrochars than single aromatic rings in lignin, with aromatic C more than two bonds away from two protons on average; and (3) the aromatic C in these hydrochars relatively less than three bonds away from three protons, on average.

Our results also demonstrate that the conclusions on ring condensation based on H/C ratios alone may not be valid. For example, Hammes et al.[33] and Schimmelpfennig and Glaser[14] proposed that a H/C ratio of ≥0.7 indicated noncondensed aromatic structures such as lignin. These four water hydrochars studied had H/C ratios of 1.0−1.2 but contained more condensed aromatic structures than lignin. This is because bulk elemental analysis is limited in differentiating structures with similar molecular formulas, which occupy the same compositional space in a van Krevelen plot.[34]

Biological and Chemical Oxygen Demand Measurements. The oxygen demands due to chemical oxidation (COD) as well as biochemical oxidation (BOD) of the feedstocks and the hydrochars were measured to estimate their potential biodegradability in the environment. BOD/COD ratios were calculated from these data (Figure 7). Whereas the COD measurements can be expected to oxidize the solid particles, giving an indication of potential oxygen demand, the BOD results measured over a period of 5 days are likely to be governed by the degradability of organic compounds desorbing in water from the solid hydrochar particles, indicating the degree of readily degradable carbon associated with the hydrochars.

The values for the COD of the sugar beet and bark feedstocks were similar and relatively low compared to the hydrochars (Figure 7). These increased as the processing temperature increased for the water hydrochars. This is consistent with the elemental analysis that showed both oxygen loss and C content increase with reaction temperature (Table 2), as well as with the NMR results that showed decreases in oxidized groups such as carbohydrates (Figure 5). As C became more enriched in the hydrochars, more C was available to be oxidized, accounting for the increased COD with increasing processing temperature. The longer reaction time appeared to have little impact on the COD of the hydrochars prepared at

dx.doi.org/10.1021/jf402345k | J. Agric. Food Chem. 2013, 61, 9401−9411

250 °C at 3 and 20 h. The slight decrease in COD for the bark hydrochar at 20 h is probably due to more aromatic structures, which are less oxidizable in COD measurements.

The results for the steam hydrochars deviated from these trends. On the basis of solid-phase C content, the COD value of steam hydrochars is expected to be close to those of the W-HTC generated at 250 °C. However, the CODs associated with steam hydrochars were lower than those produced in water at 200 °C and closer to those of the originial feedstock. This is consistent with the NMR results, though, that steam hydrochars were most similar among all of the hydrochars in their spectral features to their feedstocks. This also supports the finding that sugar beet and bark underwent deeper carbonization in water media than in steam media (at the same temperature and time).

The BOD measurements of the feedstocks produced expected results; the sugar beet feedstock had a 10-fold higher BOD than the bark (Figure 7). Bark contained appreciable aromatic content, resulting in a lower amount of soluble biodegradable C than the carbohydrate-dominated sugar beet. The carbonization of the feedstocks produced different results, depending on their original degradability. Reaction temperature and medium had little impact on the BOD of the sugar beet hydrochar suspensions (Figure 7), despite changes in the hydrochar composition. Only the extension of the reaction time to 20 h caused a substantial decrease in BOD. The hydrochar carbonized in steam, however, had a BOD/COD ratio similar to that of the original feedstock. These results are likely governed by the amount as well as the biodegradability of water-soluble compounds located in the hydrochar.

In contrast, the low BOD value of the bark feedstock due to its higher aromatic C (lignin) content was increased through the HTC process, likely due to the release of degradable compounds. The presence of lignin within bark creates a barrier to hydrolysis of cellulose. The HTC process disrupts the lignocellosic structure, exposing cellulose/hemicellulose to microbial degradation. The steam carbonization produced a char with a higher degree of biodegradable compounds, with a BOD 5 times higher than that of the bark feedstock and double that of the bark water hydrochar at similar conditions. This also correlates with the BOD/COD ratios, which were low and relatively constant for all processing conditions except for the steam carbonization. The degradable compounds remained associated with the steam hydrochar, whereas in the water−carbonization process they dissolve into processing water. In water HTC, this loss to process water accounts for approximately 20% of the original carbon.[8] However, the biodegradability of bark hydrochars remained only approximately half that of the sugar beet hydrochars. As temperature was increased in the water medium to 250 °C for 3 h, the BOD of the hydrochar increased. The lengthening of reaction time from 3 to 20 h at 250 °C, however, decreased the BOD, similar to the behavior seen with the sugar beet hydrochars. No strong correlation was observed between BOD data and abundances of different functional groups.

These COD and BOD results are dependent on HTC processing conditions and likely also on the type of hydrochar postprocessing. The compounds that are solubilized during the HTC process can adsorb or remain on the surface of the hydrochars. Methods that analyze only the char as a whole will be affected by whether these soluble compounds remain on the char and therefore may not give a true picture of the hydrochars themselves. For instance, washing hydrochars with acetone has been shown to remove the soluble intermediates deposited on the hydrochar.[23] When the char stability in soil incubation tests is measured, the initial results may reflect the degradability of adsorbed compounds, rather than the whole char structure itself. The use of a BOD measurement appears promising as a supplementary test to learn more about char stability.

Effects of Biomass Type and Processing Conditions on Hydrochar Structures. The HTC processing of sugar beet and bark involved the depletion of carbohydrate C and the formation and/or enrichment of aromatic C, as well as increases of alkyl and carbonyl C. These structural changes are driven by reactions such as hydrolysis, dehydration, decarboxylation, aromatization, and recondensation.[7,35] Structural characteristics of hydrochars are shown to depend on feedstock type, the phase of the reaction medium, processing temperature, and time.

Feedstock type plays a significant role in hydrochar composition. The dominance of cellulose/hemicellulose in sugar beet is consistent with its high H/C and O/C ratios, whereas the presence of lignin in bark shifts it to much lower H/C and O/C ratios relative to sugar beet. Falco et al.[21] compared the structural differences between glucose-, cellulose-, and lignocellulosic biomass-derived HTC materials. Whereas the cellulose signals of glucose- and cellulose-based hydrochars were lost at 200 °C, they were present in the spectrum of rye straw-based material up to 200 °C. This difference was attributed by the authors to the presence of lignin in rye straw, which might stabilize the cellulose and prevent the disruption of its crystalline structure at lower temperatures. In the present study, however, characteristic peaks of cellulose were distinct in the spectra of both sugar beet and bark hydrochars prepared at 200 °C. This suggests that sugar beet contains carbohydrates (other than cellulose) that decompose at higher temperature. The main structural difference between sugar beet and bark hydrochars lies in the presence of lignin residues in the bark hydrochars. Consistent with our finding, lignin has been shown to be affected by HTC processing to a very limited extent and retained in hydrochars.[21,24] Hence, the aromaticity of the bark started out at a higher level than that of the sugar beet feedstock (which is essentially zero) due to the presence of lignin and remained higher in the bark hydrochars produced at the same process conditions as the sugar beet hydrochars. This is consistent with lower H/C ratios of bark hydrochars than those of corresponding sugar beet hydrochars, except for those prepared at 200 °C for 3 h during water HTC. The extended carbonization at 250 °C for 20 h increased the aromaticity of the bark hydrochar to 64%, whereas the sugar beet hydrochar under this condition remained below 53%. The presence of lignin also resulted in a much lower BOD of bark and increasing trends of BOD after HTC processing.

Although both time and temperature influence hydrochar characteristics, temperature is the decisive factor. HTC at higher temperatures (250 °C) produced water hydrochars that were more aromatic and were almost completely depleted of carbohydrates, consistent with their lower H/C and O/C ratios. In the case of sugar beet hydrochars, those prepared at 250 °C showed lower O/C but higher H/C ratios, suggesting the significance of decarboxylation. Increasing the residence time from 3 to 20 h at 250 °C at most led to the enrichment of nonprotonated aromatic C−C in sugar beet and bark hydrochars (Figure 5), confirming the shift of their H/C ratios to lower values.

Both bark and sugar beet underwent deeper carbonization during the water HTC (200 °C, 3 h) than during the steam HTC process (200 °C, 3 h), because the increase of aromatic and alkyl C and decrease of carbohydrate C were more prominent in W-HTC hydrochars. This effect was much more evident for sugar beet hydrochars. These results are contrary to those found using the common interpretation of elemental analysis via the van Krevelen plot. The steam hydrochars were located at considerably lower H/C values on the plot than the corresponding water hydrochars, implying a more carbonized structure of steam hydrochars. We speculate that reactions leading to the production of methane (demethylation), which has been reported to be of minor importance during water HTC,[24] might become significant during steam HTC. The significant loss of CH_4 in steam hydrochars would explain their remarkably lower H/C ratios.

Further differences caused by the reaction medium were found in the biodegradability tests. Whereas the HTC process increased the degradability of the bark in both steam and water, the steam hydrochar from bark showed a BOD double that of the bark water hydrochar under similar conditions. The difference may be related to the fact that the degradable compounds, which could have been washed away with the process water during water HTC, were retained in the steam hydrochars.

AUTHOR INFORMATION

Corresponding Author

*(J.M.) E-mail: maojd@njau.edu.cn or jmao@odu.edu. Phone: (757) 683-6874. Fax: (757) 683-4628.

Funding

We thank the National Science Foundation (CBET-0853950) for financial support.

Notes

The authors declare no competing financial interest.

ACKNOWLEDGMENTS

Collaboration with the USDA-ARS was conducted according to Agreement NFCA 6657-13630-004-01N. We are grateful to R. Schlitt for provision of the first larger scale produced German hydrochar samples. Mention of trade names or commercial products is solely for the purpose of providing specific information and does not imply recommendation or endorsement by the U.S. Department of Agriculture. We thank Editor Dr. James N. Seiber and the four anonymous reviewers for their comments that helped to improve the presentation of this work.

REFERENCES

(1) Glaser, B.; Haumaier, L.; Guggenberger, G.; Zech, W. The 'Terra Preta' phenomenon: a model for sustainable agriculture in the humid tropics. *Naturwissenschaften* **2001**, *88*, 37−41.

(2) Lehmann, J.; Czimczik, C. I.; Laird, D. A.; Sohi, S., Stability of biochar in soil. In *Biochar for Environmental Management: Science and Technology*, Lehmann, J., Joseph, S., Eds.; Routledge, Taylor and Francis: Florence, KY, 2009; pp 183−205.

(3) Mao, J. D.; Johnson, R. L.; Lehmann, J.; Olk, D. C.; Neves, E. G.; Thompson, M. L.; Schmidt-Rohr, K. Abundant and stable char residues in soils: implications for soil fertility and carbon sequestration. *Environ. Sci. Technol.* **2012**, *46*, 9571−9576.

(4) Lehmann, J.; Joseph, S. *Biochar for Environmental Management: Science and Technology*; Routledge, Taylor and Francis: Florence, KY, 2009.

(5) Whitman, T.; Lehmann, J. Biochar − one way forward for soil carbon in offset mechanisms in Africa? *Environ. Sci. Policy* **2009**, *12*, 1024−1027.

(6) Tang, J.; Zhu, W.; Kookana, R.; Katayama, A. Characteristics of biochar and its application in remediation of contaminated soil. *J. Biosci. Bioeng.* **2013**, DOI: 10.1016/j.jbiosc.2013.05.035.

(7) Funke, A.; Ziegler, F. Hydrothermal carbonization of biomass: a summary and discussion of chemical mechanisms for process engineering. *Biofuels, Bioprod. Biorefin.* **2010**, *4*, 160−177.

(8) Libra, J. A.; Ro, K. S.; Kammann, C.; Funke, A.; Berge, N. D.; Neubauer, Y.; Titirici, M.-M.; Fühner, C.; Bens, O.; Kern, J.; Emmerich, K.-H. Hydrothermal carbonization of biomass residuals: a comparative review of the chemistry, processes and applications of wet and dry pyrolysis. *Biofuels* **2010**, *2*, 71−106.

(9) Schuhmacher, J. P.; Huntjens, F. J.; Vankrevelen, D. W. Chemical structure and properties of coal. 26. Studies on artificial coalification. *Fuel* **1960**, *39*, 223−234.

(10) Bergius, F. *Die Anwendung hoher Drücke bei chemischen Vorgängen und eine Nachbil dung des Entstehungsprozesses der Steinkohle*; Wilhelm Knapp: Halle an der Saale, Germany, 1913; pp 41−58.

(11) Fuertes, A. B.; Arbestain, M. C.; Sevilla, M.; Macia-Agullo, J. A.; Fiol, S.; Lopez, R.; Smernik, R. J.; Aitkenhead, W. P.; Arce, F.; Macias, F. Chemical and structural properties of carbonaceous products obtained by pyrolysis and hydrothermal carbonisation of corn stover. *Aust. J. Soil Res.* **2010**, *48*, 618−626.

(12) Sugimoto, Y.; Miki, Y. In *Chemical Structure of Artificial Coals Obtained from Cellulose, Wood and Peat*; Ziegler, A., van Heek, K. H., Klein, J., Wanzl, W., Eds.; Druck und Verlag GmbH: Essen, Germany, 1997; pp 187−190.

(13) Kammann, C.; Ratering, S.; Eckhard, C.; Muller, C. Biochar and hydrochar effects on greenhouse gas (carbon dioxide, nitrous oxide, and methane) fluxes from soils. *J. Environ. Qual.* **2012**, *41*, 1052−1066.

(14) Schimmelpfennig, S.; Glaser, B. One step forward toward characterization: some important material properties to distinguish biochars. *J. Environ. Qual.* **2012**, *41*, 1001−1013.

(15) Sevilla, M.; Fuertes, A. B. The production of carbon materials by hydrothermal carbonization of cellulose. *Carbon* **2009**, *47*, 2281−2289.

(16) Sevilla, M.; Fuertes, A. B. Chemical and structural properties of carbonaceous products obtained by hydrothermal carbonization of saccharides. *Chem.−Eur. J.* **2009**, *15*, 4195−4203.

(17) Titirici, M. M.; Antonietti, M. Chemistry and materials options of sustainable carbon materials made by hydrothermal carbonization. *Chem. Soc. Rev.* **2010**, *39*, 103−116.

(18) Rillig, M. C.; Wagner, M.; Salem, M.; Antunes, P. M.; George, C.; Ramke, H. G.; Titirici, M. M.; Antonietti, M. Material derived from hydrothermal carbonization: effects on plant growth and arbuscular mycorrhiza. *Appl. Soil Ecol.* **2010**, *45*, 238−242.

(19) Berge, N. D.; Ro, K. S.; Mao, J.; Flora, J. R. V.; Chappell, M. A.; Bae, S. Hydrothermal carbonization of municipal waste streams. *Environ. Sci. Technol.* **2011**, *45*, 5696−5703.

(20) Baccile, N.; Laurent, G.; Babonneau, F.; Fayon, F.; Titirici, M. M.; Antonietti, M. Structural characterization of hydrothermal carbon spheres by advanced solid-state MAS C-13 NMR investigations. *J. Phys. Chem. C* **2009**, *113*, 9644−9654.

(21) Falco, C.; Baccile, N.; Titirici, M. M. Morphological and structural differences between glucose, cellulose and lignocellulosic biomass derived hydrothermal carbons. *Green Chem.* **2011**, *13*, 3273−3281.

(22) Falco, C.; Perez Caballero, F.; Babonneau, F.; Gervais, C.; Laurent, G.; Titirici, M.-M.; Baccile, N. Hydrothermal carbon from biomass: structural differences between hydrothermal and pyrolyzed carbons via ^{13}C solid state NMR. *Langmuir* **2011**, *27*, 14460−14471.

(23) Cao, X. Y.; Ro, K. S.; Chappell, M.; Li, Y. A.; Mao, J. D. Chemical structures of swine-manure chars produced under different carbonization conditions investigated by advanced solid-state C-13 nuclear magnetic resonance (NMR) spectroscopy. *Energy Fuels* **2011**, *25*, 388−397.

(24) Dinjus, E.; Kruse, A.; Troger, N. Hydrothermal carbonization − 1. Influence of lignin in lignocelluloses. *Chem. Eng. Technol.* **2011**, *34*, 2037−2043.
(25) Titirici, M. M.; Thomas, A.; Yu, S. H.; Muller, J. O.; Antonietti, M. A direct synthesis of mesoporous carbons with bicontinuous pore morphology from crude plant material by hydrothermal carbonization. *Chem. Mater.* **2007**, *19*, 4205−4212.
(26) Standard Test Methods for Proximate Analysis of the Analysis Sample of Coal and Coke by Instrumental Procedures, ASTM International, West Conshohocken, PA, 2009.
(27) Mao, J. D.; Chen, N.; Cao, X. Y. Characterization of humic substances by advanced solid state NMR spectroscopy: demonstration of a systematic approach. *Org. Geochem.* **2011**, *42*, 891−902.
(28) Dixon, W. T. Spinning-sideband-free and spinning-sideband-only NMR spectra in spinning samples. *J. Chem. Phys.* **1982**, *77*, 1800−1809.
(29) van Krevelen, D. W. Graphical-statistical method for the study of structure and reaction processes of coal. *Fuel* **1950**, *29*, 269−284.
(30) Chun, Y.; Sheng, G. Y.; Chiou, C. T.; Xing, B. S. Compositions and sorptive properties of crop residue-derived chars. *Environ. Sci. Technol.* **2004**, *38*, 4649−4655.
(31) Chuntanapum, A.; Matsumura, Y. Formation of tarry material from 5-HMF in subcritical and supercritical water. *Ind. Eng. Chem. Res.* **2009**, *48*, 9837−9846.
(32) Mao, J. D.; Schmidt-Rohr, K. Recoupled long-range C-H dipolar dephasing in solid-state NMR, and its use for spectral selection of fused aromatic rings. *J. Magn. Reson.* **2003**, *162*, 217−227.
(33) Hammes, K.; Smernik, R. J.; Skjemstad, J. O.; Herzog, A.; Vogt, U. F.; Schmidt, M. W. I. Synthesis and characterisation of laboratory-charred grass straw (*Oryza sativa*) and chestnut wood (*Castanea sativa*) as reference materials for black carbon quantification. *Org. Geochem.* **2006**, *37*, 1629−1633.
(34) Podgorski, D. C.; Hamdan, R.; McKenna, A. M.; Nyadong, L.; Rodgers, R. P.; Marshall, A. G.; Cooper, W. T. Characterization of pyrogenic black carbon by desorption atmospheric pressure photoionization Fourier transform ion cyclotron resonance mass spectrometry. *Anal. Chem.* **2012**, *84*, 1281−1287.
(35) Peterson, A. A.; Vogel, F.; Lachance, R. P.; Froling, M.; Antal, M. J.; Tester, J. W. Thermochemical biofuel production in hydrothermal media: a review of sub- and supercritical water technologies. *Energy Environ. Sci.* **2008**, *1*, 32−65.
(36) Sutton, M. D.; Peterson, J. B. D. Fermentation of sugarbeet pulp for ethanol production using bioengineered *Klebsiella oxytoca* strain P2. *J. Sugar Beet Res.* **2001**, *38*, 19−34.
(37) Kraft, R. *Zur chemisch-technologischen Verwertung von*; Cuvillier Verlag: Göttingen, Germany, 2006.
(38) Chen, S.; Wen, Z.; Liao, W.; Liu, C.; Kincaid, R.; Harrison, J.; Elliott, D. C.; Brown, M. D.; Stevens, D. J. Studies into using manure in a biorefinery concept. *Appl. Biochem. Biotechnol.* **2005**, *124*, 999−1015.
(39) Mao, J. D.; Schmidt-Rohr, K. Accurate quantification of aromaticity and nonprotonated aromatic carbon fraction in natural organic matter by ^{13}C solid-state nuclear magnetic resonance. *Environ. Sci. Technol.* **2004**, *38*, 2680−2684.